文章编号:2095-1922(2020)03-0536-07 doi:10.11717/j.issn:2095-1922.2020.03.19

惯性式振动机过渡过程的动态响应分析

侯祥林[1],伍丹霞[1],刘铁林[2]

(1. 沈阳建筑大学机械工程学院,辽宁 沈阳 110168;2. 沈阳建筑大学土木工程学院,辽宁 沈阳 110168)

摘 要 **目的** 研究单轴惯性振动机过共振区的振动振幅在起动和停车过程中的变化规律,确定振动系统在振动过程中的共振时的最大振幅,解决具有三自由度的振动机起停过程的偏心块转动量、振动机位移与速度变量随时间的变化问题. **方法** 以振动力学为基础,对单轴惯性振动机在过渡过程中,建立振动系统动力学模型,采用将龙格-库塔法数值积分方法和解析法相结合的方法,对惯性振动机起动与停车过程中的偏心块角速度、主振动方向位移和速度变化进行编制程序. **结果** 在起振过程中的共振时的理论幅值与实测共振幅值相差0.000 44 m,在停车过程中系统共振时的幅值与实测共振时的幅值相差为0.000 5 m,理论分析结果与实测结果十分接近. **结论** 对单轴惯性振动系统建立的理论推导与实际工作状况符合,可为惯性振动系统共振中振幅研究提供有效的理论依据.

关键词 惯性振动机;过渡过程;龙格-库塔法;振动响应

中图分类号 TH13.1 **文献标志码** A

Dynamic Responses of Inertial Vibrating Machine in Transient Processes

HOU Xianglin[1], *WU Danxia*[1], *LIU Tielin*[2]

(1. School of Mechanical Engineering, Shenyang Jianzhu University, Shenyang, China, 110168; 2. School of Civil Engineering, Shenyang Jianzhu University, Shenyang, China, 110168)

Abstract: This paper was proposed to study the vibration amplitude changes of a single-axis inertial vibrator passing through a resonance zone at the starting and shutdown stages, and determine the maximum resonance amplitude of the vibration system in the process of vibration, which resolve a three-degree-of-freedom problem that including the eccentric block rotation, vibrator displacement, and the velocity variables of vibrator. On the basis of vibration mechanics, a dynamics model of vibration system was built for the single-axis inertial vibrator in the transient process. Also, Runge-Kutta numerical integration and analytic methods were combined to program the angular velocity of eccentric blocks, displacement along the main

收稿日期:2018-09-15
基金项目:国家自然科学基金项目(11672190)
作者简介:侯祥林(1962—),男,教授,博士,从事机械动力学方面研究.

vibration direction, and speed variation of the inertial vibrator in the process of startup and shutdown. In the process of initial vibration, a difference of 0.00044m in amplitude is determined between the theoretical resonance amplitude and the measured resonance amplitude, while in the shutdown process, a difference of 0.0005m is determined between the system resonance amplitude and the measured resonance amplitude. The theoretical analysis results and the measured results are found closely approximate. The theoretical derivation established for the single-axis inertial vibration system tallies with its practical work state, thus qualified to be a valid theoretical basis for studies of resonance vibration amplitude of inertial vibration systems.

Key words: inertial vibration machine; transient process; Runge-Kutta method; vibration response

振动筛普遍应用于工业部门的机械设备,其工作原理涉及振动等力学领域,在冶金等领域大量应用.振动机在过渡过程期间,由于要过共振区时,当激振频率与固有频率相同时,此时振幅的幅值会比正常工作时候的幅值远远高出,关于这方面的研究,目前国内许多学者对共振理论进行了大量研究,并为减小过共振区的振幅的幅值的变化问题提出理论和解决措施[1-3].顾大卫,闻邦椿等[4-7]以实验测试方法绘制了单轴惯性振动机的响应曲线,并给出了求解摩擦阻矩求法和阻力系数的近似表达式.胡广深等[8]提出了非周期性激振力振动系统响应的杜哈梅积分求解方法以及在振动筛在起动和停车过程的减振问题中通过实测结果给出振幅的变化范围,提出有效控制方法和实测起动过程摩擦阻力矩的近似表达式.文献[9-17]对振动筛进行了大量的实验和参数分析,研究结果为振动筛的工程应用提供参考.李叶[18],邱明[19],侯祥林[20]对振动过程进行研究分析以及对相应的参数的动态变化对振幅的影响,与实测结果相符.

基于此,笔者以结构动力学分析为基础,根据振动力学以及数值分析列出方程并进行数值求解,分析惯性振动系统在振动过程中的瞬态变化,得出振幅在起停过程中的幅值的变化情况.对单轴惯性振动系统建立的理论推导与实际工作状况符合,为惯性振动系统共振中振幅研究提供有效的理论依据.

1　惯性式振动机过渡过程动力学分析

1.1　单轴惯性振动机振动方程

(1)力学模型

单轴惯性振动机力学模型如图 1 所示,振动机质量为 M,偏心块转动中心为 O,偏心块质量为 m,阻尼系数为 f_x,f_y,刚度系数为 k_x,k_y.它是 3 自由度振动问题,x,y,φ 分别为振动中心 O 的横向的位移,纵向的位移和偏心块转动的转角.

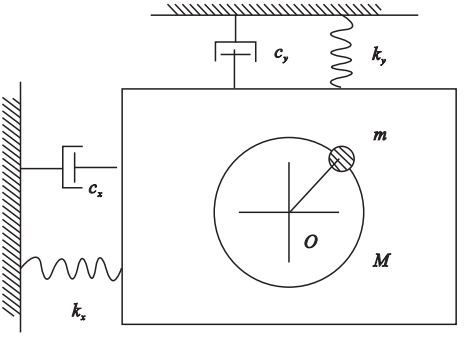

图 1　力学模型

Fig. 1　Dynamic model

(2)微分方程

图 2 为振动机力学模型.其中,$M\ddot{x}$,$M\ddot{y}$,$m\ddot{x}$,$m\ddot{y}$,Q_m^n,Q_m^τ 为惯性力,$Q_m^n = m\dot{\varphi}^2 r$,$Q_m^\tau = m\ddot{\varphi} r$.$f_x\dot{x}$,$f_y\dot{y}$ 为阻尼力;$k_x x$,$k_y y$ 为弹性力.图 3 为偏心块受力图.其中,DMO 为电机驱动力偶;DMf 为阻力偶;I 为偏心质量对转轴的转动惯量.

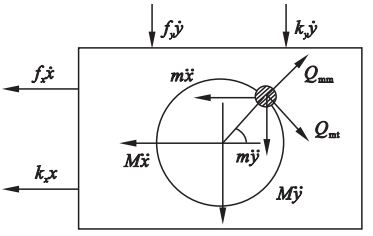

图2 振动机模型受力分析图

Fig. 2 Loading analysis diagram of vibrating machine model

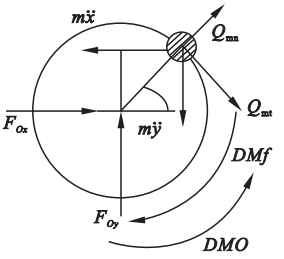

图3 偏+心块局部受力分析图

Fig. 3 Local force analysis of eccentric block

(3)单轴惯性振动机微分方程

应用达朗贝尔原理,可以建立单轴惯性振动机微分方程为

$$\begin{cases} M_0\ddot{y}+f_y\dot{y}+k_y y = mr\dot{\varphi}^2\sin\varphi - mr\ddot{\varphi}\cos\varphi, \\ M_0\ddot{x}+f_x\dot{x}+k_x x = mr\dot{\varphi}^2\cos\varphi + mr\ddot{\varphi}\sin\varphi - \\ mr\ddot{x}\sin\varphi + mr\ddot{y}\cos\varphi + I\ddot{\varphi} = DMO - \\ DMf - mgr\cos\varphi. \end{cases} \tag{1}$$

其中,$M_0 = M + m$.

1.2 微分方程的状态方程化

为采用数值程序分析求解,将式(1)视为$\ddot{x},\ddot{y},\ddot{\varphi}$的线性方程组,应用克莱姆法求解.

$$\Delta = \begin{vmatrix} 0 & M_0 & mr\cos\varphi \\ M_0 & 0 & -mr\sin\varphi \\ -mr\sin\varphi & mr\cos\varphi & I \end{vmatrix} = M_0 m^2 r - M_0{}^2 I. \tag{2}$$

$$\Delta_x = \begin{vmatrix} mr\dot{\varphi}^2\sin\varphi - f_y\dot{y} - k_y y & M_0 & mr\cos\varphi \\ mr\dot{\varphi}^2\cos\varphi - f_x\dot{x} - k_x x & 0 & -mr\sin\varphi \\ DMO - DMf - mrg\cos\varphi & mr\cos\varphi & I \end{vmatrix} = mr\cos\varphi(m\dot{\varphi}^2 r\cos\varphi - f_x\dot{x} + k_x x) - M_0 mr\sin\varphi$$

$$(DMO - DMf - mrg\cos\varphi) + mr\sin\varphi\cos\varphi(mr\dot{\varphi}^2\sin\varphi - f_y\dot{y} - k_y y) - IM(mr\dot{\varphi}^2\cos\varphi - f_x\dot{x} - k_x x). \tag{3}$$

$$\Delta_y = \begin{vmatrix} 0 & mr\dot{\varphi}^2\sin\varphi - f_y\dot{y} - k_y y & mr\cos\varphi \\ M_0 & mr\dot{\varphi}^2\cos\varphi - f_x\dot{x} - k_x x & -mr\sin\varphi \\ -mr\sin\varphi & DMO - DMf - mrg\cos\varphi & I \end{vmatrix} = M_0 mr\cos\varphi\,(DMO - DMf - mrg\cos\varphi) + mr\sin\varphi\,(mr\dot{\varphi}^2\sin\varphi - f_y\dot{y} - k_y y) + mr\sin\varphi\cos\varphi\,(mr\dot{\varphi}^2\cos\varphi - f_x\dot{x} - k_x x) - IM(mr\dot{\varphi}^2\sin\varphi - f_y\dot{y} - k_y y). \tag{4}$$

$$\Delta_\varphi = \begin{vmatrix} 0 & M_0 & mr\dot{\varphi}^2\sin\varphi - f_y\dot{y} - k_y y \\ M_0 & 0 & mr\dot{\varphi}^2\cos\varphi - f_x\dot{x} - k_x x \\ -mr\sin\varphi & mr\cos\varphi & DMO - DMf - mrg\cos\varphi \end{vmatrix} = M_0 mr\cos\varphi(mr\dot{\varphi}^2\sin\varphi - f_y\dot{y} - k_y y) - mr\sin\varphi(mr\dot{\varphi}^2\cos\varphi - f_x\dot{x} - k_x x) - M_0(DMO - DMf - mrg\cos\varphi). \tag{5}$$

可得:

$$\ddot{x} = \frac{\Delta_x}{\Delta} = f_4(x,y,\varphi,\dot{x},\dot{y},\dot{\varphi}), \tag{6}$$

$$\ddot{y} = \frac{\Delta_y}{\Delta} = f_5(x,y,\varphi,\dot{x},\dot{y},\dot{\varphi}), \tag{7}$$

$$\ddot{\varphi} = \frac{\Delta_\varphi}{\Delta} = f_6(x,y,\varphi,\dot{x},\dot{y},\dot{\varphi}). \tag{8}$$

设$x = z_1, y = z_2, \varphi = z_3, \dot{x} = z_4, \dot{y} = z_5, \dot{\varphi} = z_6$,则获得可采用数值程序计算的状态方程:

$$\begin{cases} \dot{z}_1 = z_4, \\ \dot{z}_2 = z_5, \\ \dot{z}_3 = z_6, \\ \dot{z}_4 = f_4(z_1,z_2,z_3,z_4,z_5,z_6), \\ \dot{z}_5 = f_5(z_1,z_2,z_3,z_4,z_5,z_6), \\ \dot{z}_6 = f_6(z_1,z_2,z_3,z_4,z_5,z_6). \end{cases} \tag{9}$$

2　单轴惯性振动机过渡过程分析

2.1　起动过程响应数值求解

(1)起动第一阶段

偏心块开始转动,转速增加到稳定转速,此时系统有 3 自由度,按状态方程(9)分析,用 Runge-kutta 数值积分法编程求解,程序框图如图 4 所示. 设时间 $t=0$ 时,对应状态量 $z_i(i=1,2,3,4,5,6)$,对应 $x(0)$,$y(0)$,$\varphi(0)$,$\dot{x}(0)$,$\dot{y}(0)$,$\omega(0)$,程序计算判断转速达到稳定为结束条件,$|\Delta\omega|<e_1$,此时,$t_1=t_{20}$,所对应状态为 x_{20},y_{20},φ_{20},$\dot{x}_{20}$,$\dot{y}_{20}$,ω_{20}.

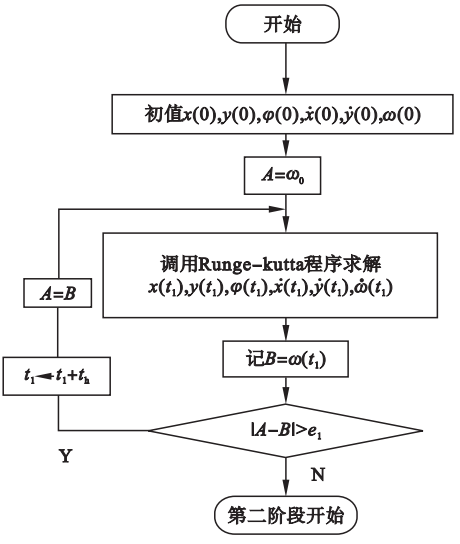

图 4　起动阶段程序框图

Fig. 4　Flow chart of starting stage

(2)起动第二阶段

偏心块达到稳定转速后,开始进入有自由衰减项的强迫振动,此时振动系统自由振动和强迫振动,自由振动逐渐衰减,达到稳定强迫振动. 由式(1),该阶段微分方程为 2 个自由度方程. 其初始条件为 x_{20},y_{20},φ_{20},$\dot{x}_{20}$,$\dot{y}_{20}$,ω_{20}.

$$\begin{cases} M_0\ddot{x}+f_x\dot{x}+k_x x=m\omega^2 r\cos(\omega t_2+\varphi_{20}), \\ M_0\ddot{y}+f_y\dot{y}+k_y y=m\omega^2 r\sin(\omega t_2+\varphi_{20}). \end{cases} \tag{10}$$

令 $p_y=\sqrt{\dfrac{k_y}{M_0}}$,$n_y=\dfrac{f_y}{2M_0}$,$z_y=\dfrac{\omega}{p_y}$,$\zeta_y=\dfrac{n_y}{p_y}$

$p_{ry}=\sqrt{p_y^2-n_y^2}$.

设:$y=\mathrm{e}^{-n_y t_2}(A_1\cos p_{ry}t_2+A_2\sin p_{ry}t_2)$

可得:

$$y'=\frac{m\omega^2 r}{k_y}\frac{1}{\sqrt{(1-z_y^2)^2+4\zeta_y^2 z_y^2}}\sin(\omega t_2+\varphi_{20}-\psi_y'),$$

$B_y=\dfrac{m\omega^2 r}{k_y}\dfrac{1}{\sqrt{(1-z_y^2)^2+4\zeta_y^2 z_y^2}}$,$\psi_y'=\tan^{-1}\dfrac{2\zeta_y z_y}{1-z_y^2}$,$\psi_y=\psi_y'-\varphi_{20}$,$Y=y+y'=\mathrm{e}^{-n_y t_1}(A_1\cos p_{ry}t_2+A_2\sin p_{ry}t_2)+B_y\sin(\omega t_2-\psi_y)$,

$Y'=-n_y\mathrm{e}^{-n_y t_2}(A_1\cos p_{ry}t_2+A_2\sin p_{ry}t_2)+\mathrm{e}^{-n_y t_1}(-A_1\sin p_{ry}t_2+A_2\cos p_{ry}t_2)$.

初始条件:$Y|_{t_2=0}=y_{20}$,$Y'|_{t_2=0}=\dot{y}_{20}$.

可求出:

$A_1=y_{20}+B_y\sin\psi_y$,

$A_2=(\dot{y}_{20}+n_y A_1-B_y\omega\cos\psi_y)/p_{ry}$.

第二阶段结束,其判断条件为 $\left|\sqrt{A_1^2+A_2^2}\,\mathrm{e}^{-n_y t_2}\right|<e_2$.

2.2　停车过程分析

(1)停车第一阶段

电机传递到偏心块的 *DMO* 为零,逐渐降至为零,仍采用 Runge-kutta 为数值积分方法求解,结束条件按 $\omega<e_3$. 停车第二阶段的程序框图与图 4 相同.

(2)振动机停车第二阶段

从偏心块转速为零,自由振动衰减到停止运动. 其方程为

$$\begin{cases} M_0\ddot{x}+f_x\dot{x}+k_x x=0, \\ M_0\ddot{y}+f_y\dot{y}+k_y y=0. \end{cases} \tag{11}$$

$y=\mathrm{e}^{-n_y t_4}[A'_{y_1}\sin(p_{ry}t_4)+A'_{y_2}\cos(p_{ry}t_4)]$,

$y'=-n_y e^{-n_y t_4}[A'_{y_1}\sin(p_{ry}t_4)+A'_{y_2}\cos(p_{ry}t_4)]+\mathrm{e}^{-n_y t_4}[A'_{y_1}\cos(p_{ry}t_4)-A'_{y_2}\sin(p_{ry}t_4)]$.

初始条件:$y|_{t_4=0}=y_{40}$,$y'|_{t_4=0}=\dot{y}_{40}$.

可得到:

$A'_{y_1}=(\dot{y}_{40}+n_y y_{40})/p_{ry}$,$A'_{y_2}=y_{40}$.

停车条件:

$|y|<e_4$.

3　起停过程动力学实例分析

3.1　振动机参数

采用一组具体参数为 $M_0=47.5$ kg,$m=$

1.25 kg,y 方向和 x 方向的弹簧刚度为 k_y = 17 753.6 N/m, k_x = 0, 偏心块半径 r = 0.007 8 m, 偏心块转轴转动惯量 I = 0.025 kg·m^2,阻尼系数 $f_x = f_y = 0.05$ N·m·s^{-1},阻力矩系数 $c_1 = 0.05$, $c_2 = 0.000\ 017$,电机功率为 $P_e = 0.6$ kW,额定转速 $n_e = 1\ 200$ r/min,设时间步长为 t_h, $t_h = 0.002$ s,起停过程精度设定: $e_1 = 0.05$, $e_2 = 0.005$, $e_3 = 0.5$, $e_4 = 0.02$.

3.2 过渡过程实例分析

起动过程:起动第一阶段大约经过0.718 s,偏心块角速度 ω 达到 120 rad/s. 在共振区附近最大位移约0.004 6 m,最大速度约0.264 m/s. 起动第二阶段约持续 2.5 s,自由振动衰减到零. 起动过程角速度随时间变化如图 5 所示,y 方向的位移随时间变化如图 6 所示,$\dot{y}$ 为 y 方向速度,$\dot{y}$ 随时间变化如图 7 所示.

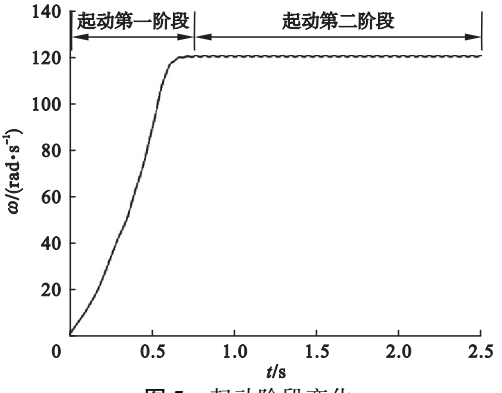

图 5 起动阶段变化

Fig. 5 ω-time curve at starting stage

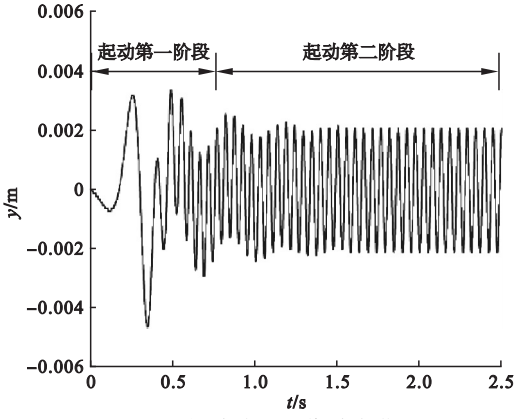

图 6 起动阶段 y 位移变化

Fig. 6 y displacement-time curve at starting stage

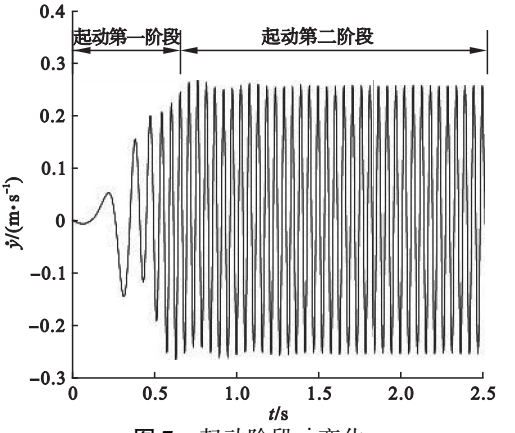

图 7 起动阶段 $\dot{y}$ 变化

Fig. 7 $\dot{y}$-time curve at starting stage

停车过程:停车第一阶段大约为14.15 s,偏心块角速度 ω 由恒定值减到0,在共振区附近最大位移约0.006 5 m,最大速度约为0.258 m/s. 停车第二阶段时间大约1.5 s,振动停止. 停车过程角速度随时间变化如图 8 所示,y 方向位移随时间变化见图9,$\dot{y}$ 为 y 方向速度,$\dot{y}$ 随时间变化见图 10.

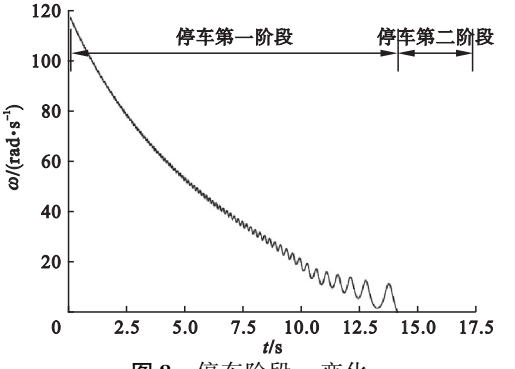

图 8 停车阶段 ω 变化

Fig. 8 ω-time curve at stopping stage

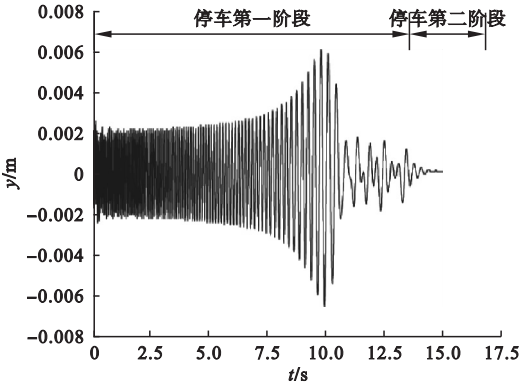

图 9 停车阶段 y 方向位移变化

Fig. 9 y displacement-time curve at stopping stage

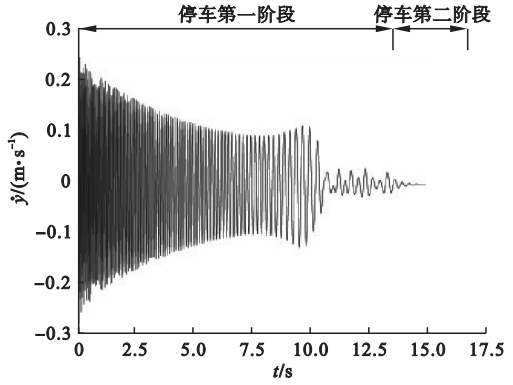

图 10　停车阶段 $\dot{y}$ 的变化

Fig. 10　$\dot{y}$ curve at stopping stage

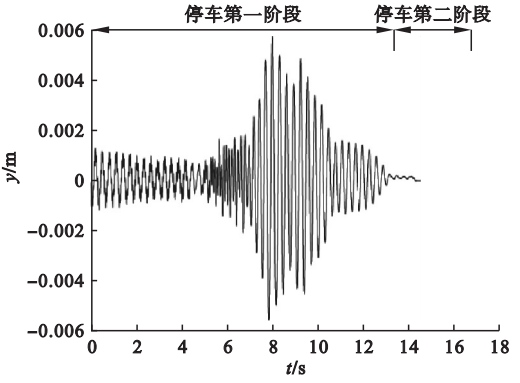

图 12　停车阶段 y 位移变化

Fig. 12　y displacement-time curve at stopping stage

4　实验结果对比分析

实测采用压电式传感器将振动信号转化为电荷信号,通过电荷放大器转化为电压信号,通过示波器检查波形,用磁带记录仪记录信号,最后通过 A/D 转化采样给微计算机离散数据. 绘制的起动、停车阶段的位移响应见图 11 和图 12 所示. 振动机起动 1. 2 s 内逐渐趋近 0. 004 16 m 左右,并且逐步趋于稳定,与理论计算分析有微小误差. 图 11 中起动第二阶段实测结果与理论分析基本一致,其幅值约 0. 001 46 m 左右,与理论分析的 0. 002 1 m 基本接近,其波动情况也相同. 图 12 中振动机停车的第一阶段振动的幅值几乎接近,图像变化趋势大致相同. 实测中 y 方向完全振动停下来所需时间与理论分析相一致.

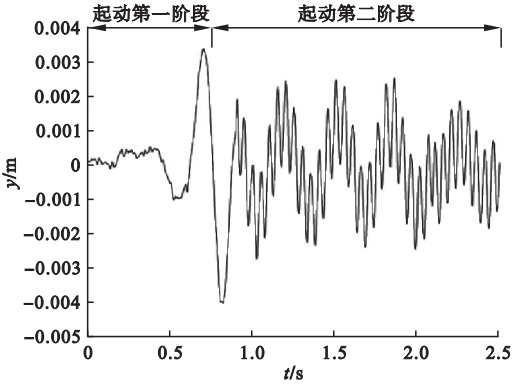

图 11　起动阶段 y 位移变化

Fig. 11　y displacement-time curve at starting stage

5　结　论

(1)共振区的幅值变化规律:惯性振动机开始振动时,幅值随着时间的变化是逐渐增加;当固有频率和激振频率相同时,振幅达到最大值,当激振频率远远超出固有频率时,振幅值反而降低,此时惯性振动系统进入工作状态.

(2)对比实测振幅值,理论分析振幅变化规律与实验结果接近,表明理论分析的正确性,其研究方法可为振动系统在过渡过程中的共振区幅值变化提供依据.

参考文献

[1]　彭利平,刘初升,王宏. 减震弹簧故障下直线筛力学模型突变研究[J]. 振动与冲击,2012,31(18):148-152.
(PENG Liping, LIU Chusheng, WANG Hong. Dynamic model catastrophe of a liner vibrating screen with damping spring fault[J]. Journal of vibration and shock, 2012, 31(18): 148-152.)

[2]　蔡萍,唐驾时. 强非线性振动系统极限环振幅控制研究[J]. 振动与冲击,2013,32(9):110-112.
(CAI Ping, TANG Jiashi. Research on limit cycle amplitude control of strong nonlinear vibration system[J]. Journal of vibration and shock, 2013, 32(9): 110-112.)

[3]　郑继明,朱伟,刘勇,等. 数值分析[M]. 北京:机械工业出版社,2016.
(ZHENG Jiming, ZHU Wei, LIU Yong, et al. Numerical analysis [M]. Beijing: China Machine Press, 2016.)

[4]　顾大卫,闻邦椿. 在振动筛上实现振动同步传动及试验研究[J]. 机械设计与制造,2018(3):4-6.

(GU Dawei, WEN Bangchun. Theory and experimental study of vibratory synchronization transmission in vibrating screen[J]. Machinery design & manufacture,2018(3):4-6.)

[5] 刘云山,张学良,闻邦椿. 双机双质体振动系统的自同步运动[J]. 中国工程机械学报,2017,15(2):95-98.
(LIU Yunshan, ZHANG Xueliang, WEN Bangchun. Self-synchronous motion of a dualmass with two motors vibrating system [J]. Chinese journal of construction machinery,2017,15(2):95-98.)

[6] 张宇飞,王延庆,闻邦椿. 轴向运动层合薄壁圆柱壳内共振的数值分析[J]. 振动与冲击,2015,34(22):82-86.
(ZHANG Yufei, WANG Yanqing, WEN Bangchun. Internal resonance of axially moving laminated thin cylindrical shells[J]. Journal of vibration and shock,2015,34(22):82-86.)

[7] 熊万里,闻邦椿,段志善. 自同步振动及振动同步传动的机电耦合机理[J]. 振动工程学报,2000,13(3):325-331.
(XIONG Wanli, WEN Bangchun, DUAN Zhishan. Mechanism of electromechanical-coupling on self-synchronous vibration and vibratory synchronization transmission [J]. Journal of vibration engineering,2000,13(3):325-331.)

[8] 胡广深,陆泽琦,陈立群. 非线性阻尼非线性刚度隔振系统参数识别[J]. 振动与冲击,2018,37(9):68-73.
(HU Guangshen, LU Zeqi, CHEN Liqun. Parametric recognition for a vibration isolation system with nonlinear stiffness and nonlinear damping[J]. Journal of vibration and shock 2018,37(9):68-73.)

[9] 王永岩,张则荣. 振动筛试验模型和原型相似试验研究[J]. 机械工程学报,2011,47(5):101-105.
(WANG Yongyan, ZHANG Zerong. Similar experimental study of test model and prototype of vibrating screen[J]. Journal of mechanical engineering,2011,47(5):101-105.)

[10] BLEKHMAN I I,FRADKOV A L,TOMCHINA O P, et al. Self-synchronization and controlled synchronization: general definition and example design [J]. Mathematics and computers in simulation,2002,58(4/5/6):367-384.

[11] WANG Boping. Eigenvalue problems in forced harmonic response analysis in structural dynamics[J]. Chinese journal of computational mechanics,2016,33(4):549-555.

[12] 贺斌,赵春雨,韩彦龙,等. 双质体振动系统的动力学参数设计方法[J]. 东北大学学报(自然科学版),2016,37(1):127-132.
(HE Bin, ZHAO Chunyu, HAN Yanlong, et al. Design method of dynamic parameters for a dual mass vibrating system[J]. Journal of northeastern university(natural science),2016,37(1):127-132.)

[13] XIAO Zhenlong, JING Xingjian, CHENG Li. The transmissibility of vibration isolators with cubic nonlinear damping under both force and base excitations [J]. Journal of sound and vibration,2013,332(5):1335-1354.

[14] 赵春雨,王得刚,张昊,等. 同向回转双机驱动振动系统的频率俘获[J]. 应用力学学报,2009,26(2):283-287.
(ZHAO Chunyu, WANG Degang, ZHANG Hao, et al. Frequency capture of vibration system with two-motor drives rotating in same direction [J]. Chinese journal of applied mechanics,2009,26(2):283-287.)

[15] XIAO Zhenlong, JING Xingjian, CHENG Li. The transmissibility of vibration isolators with cubic nonlinear damping under both force and base excitations [J]. Journal of sound and vibration,2013,332(5):1335-1354.

[16] 王得刚,赵清华,赵春雨,等. 同向回转双机驱动振动系统的自同步特性[J]. 振动·测试与诊断,2010,30(3):217-222.
(WANG Degang, ZHAO Qinghua, ZHAO Chunyu, et al. Self-synchronous feature of a vibrating system driven by two motors with the same rotation direction [J]. Journal of vibration, measurement & diagnosis, 2010, 30(3):217-222.

[17] 赵春雨,王得刚,张昊,等. 同向回转双机驱动振动系统的频率俘获[J]. 应用力学学报,2009,26(2):283-287.
(ZHAO Chunyu, WANG Degang, ZHANG Hao, et al. Frequency capture of vibration system with two-motor drives rotating in same direction [J]. Chinese journal of applied mechanics,2009,26(2):283-287.

[18] 李叶,李鹤,耿志远,等. 手持式振动机械的同步问题[J]. 振动、测试与诊断,2013,33(增刊1):9-14.
(LI Ye, LI He, GENG Zhiyuan, et al. Self-synchronization of hand-held vibrating machinery [J]. Journal of vibration, measurement & diagnosis, 2013, 33(S1):9-14.)

[19] 邱明. 大型悬挂式惯性振动设备若干关键问题研究[D]. 南京:南京理工大学,2014.
(QIU Ming. Research on several key problems of large suspension inertial vibration machine [D]. Nanjing: Nanjing University of Technology,2014.)

[20] 侯祥林. 惯性式振动机过渡过程的研究[D]. 沈阳:东北大学,1994.
(HOU Xianglin. Research on the transition process of inertial vibrating machine [D]. Shenyang:Northeastern University,1994.)

(责任编辑:刘春光 英文审校:范丽婷)